



ACOUSTICAL ANALYSIS OF ACTIVE NOISE CONTROL (ANC) SYSTEM IN A GENERAL ROOM-BASED DATA CENTER

Seyede Zahra Jalilzadeh, Mohammad Asgari

IRIB University, Tehran, Iran

e-mail: jalilzadeh@iribu.ac.ir

A walk-through survey in Data Centers indicates that it is not a safe place to work. So the customers are always seeking a new technology to reduce the acoustic noise in Data Centers. On the other hand, Active Noise Control is more advantageous in numerous applications. In this paper, we investigate the feasibility of ANC systems in data centers environment. For this purpose, a multi-channel ANC system based on FxLMS algorithm was investigated in the Islamic Republic of Iran Broadcasting (IRIB) Data Center as a room-based one. Acoustical experimental data was taken to measure the acoustic noise characteristics of frequency and Sound Pressure Level (SPL). Accordingly, the working frequency was found, the secondary paths transfer functions are determined practically. Finally, the system performance shows that the maximum Attenuation up to 12 dB was achieved by using a feed-forward multi-channel Active Noise Control system. Moreover, the results of this investigation demonstrate that Active Noise Control Systems are capable of providing acoustic noise attenuation of Data centers to improve their habitability.

1. Introduction

Islamic Republic of Iran Broadcasting (IRIB) data center, as a typical room-based ¹ data center, has a little acoustical absorption like foam or fibreglass. Main noise sources are various fans placed in servers and HVAC (Heating, Ventilation and Air Conditioning) equipment ². Active Noise Control (ANC) is an electro acoustic technology to reduce the unwanted sound by using control sources to emit inverse sound to attenuate the primary noise ³. This technology is useful especially in low frequency attenuation scenario ⁴, as Passive Noise Control (PNC) is not so effective to reduce the low frequencies.

In this paper, a feed-forward multi-channel ANC system based on FxLMS ⁵ algorithm; including 5 reference microphones, 4 control sources and 1 error microphone; was used to determine the feasibility of using active control method in data center room. Two methods were used; measured acoustical data and computational modelling. For this purpose, a multi-channel FxLMS algorithm ANC system was described in section 2. Data gathering details were explained in section 3 and the results were presented in section 4. Finally, the conclusion was outlined in section 5.

2. Multi-channel FxLMS algorithm ANC system

FxLMS⁵ is most common adaptation algorithm to update the filters' weights in ANC system. Fig. 1 shows its block diagram in a single-channel. In most applications, as there are several noise sources, the multi-channel ANC system is used inevitably⁴.

As stated before, in this paper a feed-forward multi-channel system was applied to reduce the local control of ambient noise in sample area. The multi-channel system contains $5 \times 4 \times 1$ structure.

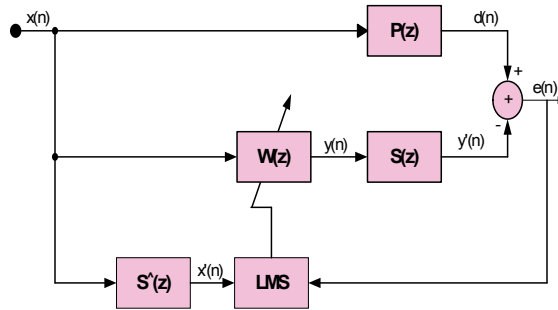


Figure 1. The block diagram of FxLMS algorithm.

Fig.2 illustrates the block diagram of a $2 \times 4 \times 1$ structure. x_1 and x_2 are the two reference signals which were captured by two reference microphones in practical experiments. The desired signal was captured by the error microphone. As Fig. 2 indicates, two reference signals according to Eq. 1 and Eq. 2, pass through the adaptive filters then through four transfer functions which are representatives of four secondary paths; the distance between error microphone and control source. Then they get together to form the total output signal to send the summation point. On the other hand, each reference signal is filtered by four estimated transfer functions as Eq. 3 and Eq. 4 state.

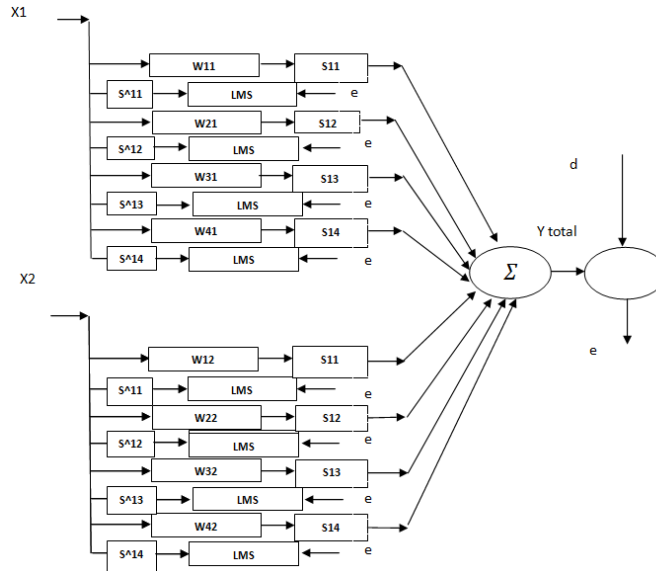


Figure 2. The block diagram of $2 \times 4 \times 1$ based on FxLMS algorithm.

$$\begin{aligned}
 y_{11} &= w_{11}(n)x_1 \\
 y_{21} &= w_{21}(n)x_1 \\
 y_{31} &= w_{31}(n)x_1 \\
 y_{41} &= w_{41}(n)x_1
 \end{aligned} \tag{1}$$

$$\begin{aligned}
 y_{12} &= w_{12}(n)x_2 \\
 y_{22} &= w_{22}(n)x_2 \\
 y_{32} &= w_{32}(n)x_2 \\
 y_{42} &= w_{42}(n)x_2
 \end{aligned} \tag{2}$$

$\hat{S}_{11}(z)$, $\hat{S}_{12}(z)$, $\hat{S}_{13}(z)$ and $\hat{S}_{14}(z)$ are the estimated transfer functions of secondary paths which were modelled here by 32-taps FIR filters.

$$\begin{aligned}
 x'_{111}(n) &= \hat{S}_{11}(n) * x_1(n) \\
 x'_{121}(n) &= \hat{S}_{12}(n) * x_1(n) \\
 x'_{131}(n) &= \hat{S}_{13}(n) * x_1(n) \\
 x'_{141}(n) &= \hat{S}_{14}(n) * x_1(n)
 \end{aligned} \tag{3}$$

Where * is the linear convolution.

$$\begin{aligned}
 x'_{211}(n) &= \hat{S}_{11}(n) * x_2(n) \\
 x'_{221}(n) &= \hat{S}_{12}(n) * x_2(n) \\
 x'_{231}(n) &= \hat{S}_{13}(n) * x_2(n) \\
 x'_{241}(n) &= \hat{S}_{14}(n) * x_2(n)
 \end{aligned} \tag{4}$$

Finally the adaptive filters weights are updated to convergence the algorithm and have the minimum residual error. The equations are given as:

$$\begin{aligned}
 w_{11}(n+1) &= w_{11}(n) + \mu x'_{111}(n) e(n) \\
 w_{21}(n+1) &= w_{21}(n) + \mu x'_{121}(n) e(n) \\
 w_{31}(n+1) &= w_{31}(n) + \mu x'_{131}(n) e(n) \\
 w_{41}(n+1) &= w_{41}(n) + \mu x'_{141}(n) e(n)
 \end{aligned} \tag{5}$$

Where μ is the adaptation step size.

$$\begin{aligned}
 w_{12}(n+1) &= w_{12}(n) + \mu x'_{121}(n)e(n) \\
 w_{22}(n+1) &= w_{22}(n) + \mu x'_{221}(n)e(n) \\
 w_{32}(n+1) &= w_{32}(n) + \mu x'_{231}(n)e(n) \\
 w_{42}(n+1) &= w_{42}(n) + \mu x'_{241}(n)e(n)
 \end{aligned}
 \tag{6}$$

3. Data Collection

Experimental data of IRIB data center was taken to measure the noise level and frequency analysis to find the powerful frequencies as well. Ten measurement locations were considered to determine the acoustic characteristics of the noise emitted by the servers and HVAC system. The transfer functions of secondary paths were modelled practically by the environment recorded sound. As stated before, IRIB data center is a reverberant room as it contains low absorbent surface such as acoustic tile or foam. It means that the sound intensity is increased by the reflection of hard surfaces like walls, monitors and so on. It makes that noise levels would be noticeable and annoying. The measurement was taken by Investigator 2260⁶ (Fig. 3).



Figure 3. Measuring the acoustic noise characteristics in IRIB data center by using investigator 2260.

AKG D880⁷, Neumann U87 Ai⁸, M-Audio Project Mixer⁹, Omni Power Sound Source Type 4296¹⁰, Power Amplifier Type 2716¹⁰ and a Dell Vostro¹¹ Lap top also were used in data gathering to form an ANC system as shown in Fig. 4.

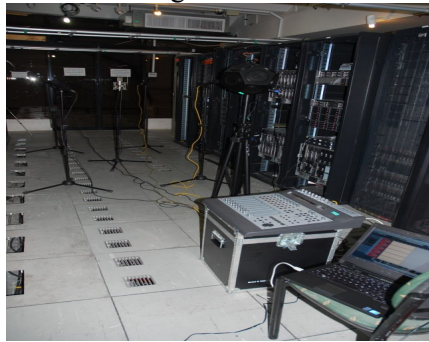


Figure 4. Experimental set up in IRIB data center.

3.1 Working Frequency

To find the error microphone location, fifteen measurement points were considered. The noise equivalent level (L_{req}) was found to vary gradually along the room's space. It means that the total SPL at A-weighting network (L_{Aeq}) of ambient noise in everylocation of room was almost identical. So keeping this mind and regarding the physical limitations to set up the equipment, the room central point was selected to place the error microphone.

It comes to find the distance between error microphone and control source. Although, the most of researches are based on trial and error to have a sensible performance, here, we determined the distance by using Eq. 7 to find the best. Investigation of sound pressure level over octave band frequencies indicated that the maximum energy belongs to frequencies lower than 1000 Hz especially about 800 Hz.

Assuming the sound velocity is 345 meter per second, we have:

$$\lambda = \frac{c}{f} = \frac{345}{800} = 0.43 \text{ m} \tag{7}$$

So the distance between the control sources and error microphone to determine the secondary paths transfer functions were selected 50 centimetres.

3.2 Secondary paths modelling

As stated in section 2, the secondary path modelling is one of the main parts of ANC system analysis. The frequency response of secondary path was illustrated in Fig. 5. The phase frequency shows that the phase delay was linear. In other word, there is no distortion between frequencies components.

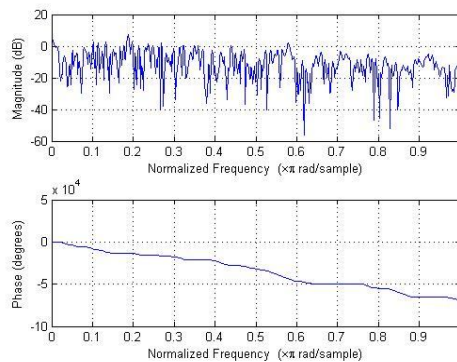


Figure 5. The frequency and phase response of secondary path of IRIB data center.

Here, four transfer functions were considered as there are four control sources. Fig.3 shows the placement of loudspeaker (control source) and the error microphone to model the secondary paths. White noise was transmitted at environment by using Omni Power Sound Source Type 4296¹⁰ and received by Neumann U87 Ai⁸ as the error microphone as shown in Fig. 6. These signals were called respectively input and output signals.

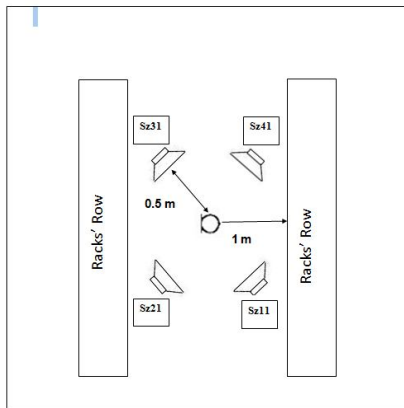


Figure 6.The placement of control sources and error microphone for data gathering to model the secondary paths.



Figure 7. The power Sound source and the error microphone for data gathering to model the scndary path.

3.2.1 Secondary paths Determination

The secondary paths were determined based on Output Error Structure model (OE) ¹² by using 1000 samples of input and output signals which is stated in previous section. The filers' types were IIR to model the acoustic paths. The optimized order of IIR filter was determined and selected eight by using signal processing toolbox as Fig. 8 shows.

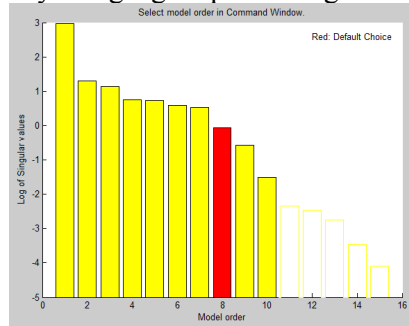


Figure 8. Selection of modelled IIR filter by using MATLAB.

3.2.2 Secondary paths Estimation

Both the input and output signals were captured and transfer functions were estimated with MATLAB ¹³ function tfestimate. The functions calculate linear time invariant transfer functions using the equation:

$$T_{xy}(f) = \frac{P_{xy}}{P_{xx}} \quad (8)$$

Where cross power spectral density of the input and output is divided with the power spectral density on the input ¹⁴. All signal processing was implemented in time domain so the impulse responses of secondary paths were achieved by using IFFT of transfer functions. Fig. 9 shows one of the secondary path impulse responses with 32 coefficients.

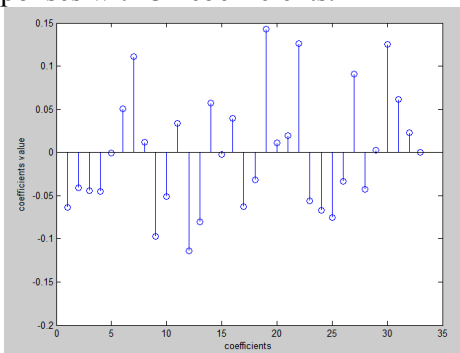


Figure 9. The Impulse Response of secondary path in IRIB data center.

Briefly, the simulation parameters were outlined in Table.1.

Table 1. Simulation Parameters in Signal Processing.

modelled Filter	Filter name	Filter type	Filter tap
Adaptive filter	$W(z)$	FIR	128 tap
Secondary paths modelling	$S(z)$	IIR	8 order
Estimated secondary paths	$\hat{S}(z)$	FIR	32 tap

3.2.3 Step Size Selection

Step size selection is an essential work in adapting processing. Here, this was based on trial and error to find the best for sensible stability and convergence of the algorithm.

For this purpose, first a scope of step size magnitudes were determined then best magnitude, 2×10^{-5} was found to achieve the most stability with.

4. Results

In this section, the system performances for multi-band frequency were presented. Fig. 10 to Fig. 12 shows the system performance. As Fig. 10 (b) illustrates, the system is not useful to attenuate the wide-band noise. Although, the performance was improved when the band-width was restricted, the system efficiency was decreased in very narrow band noise reduction as shown in Fig. 12 (b).

Among the different multi-band frequencies investigation, 500 to 2000 Hz band-width was the best band-width to noise attenuation with maximum attenuation.

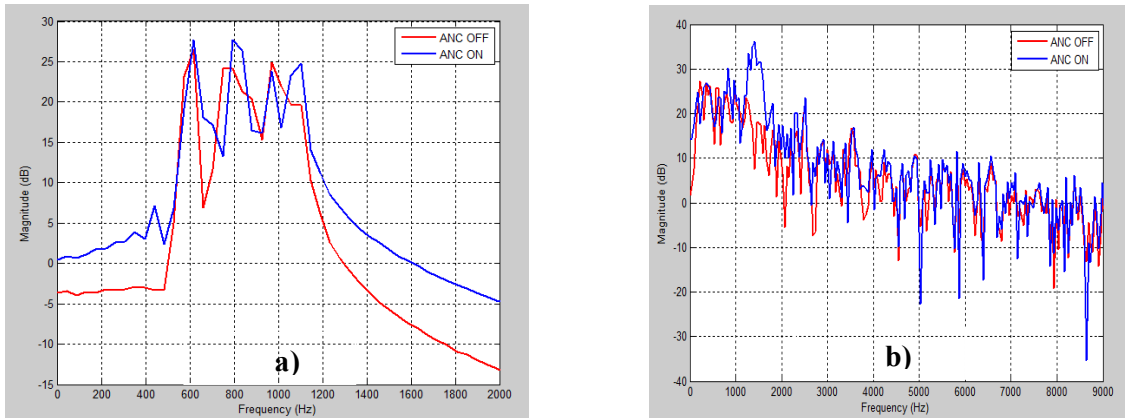


Figure 10. The system performance for band-width a) 400 to 800 Hz b) 80 to 8000 Hz.

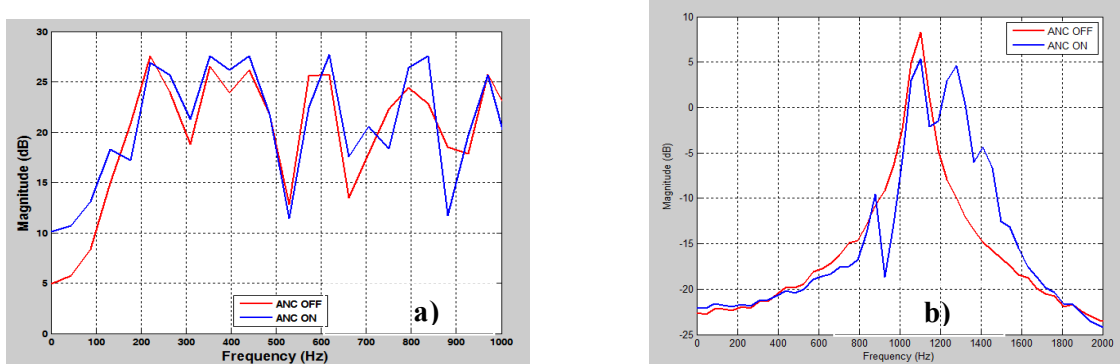


Figure 11. The system performance for band-width a) 80 to 800 Hz b) 560 to 960 Hz.

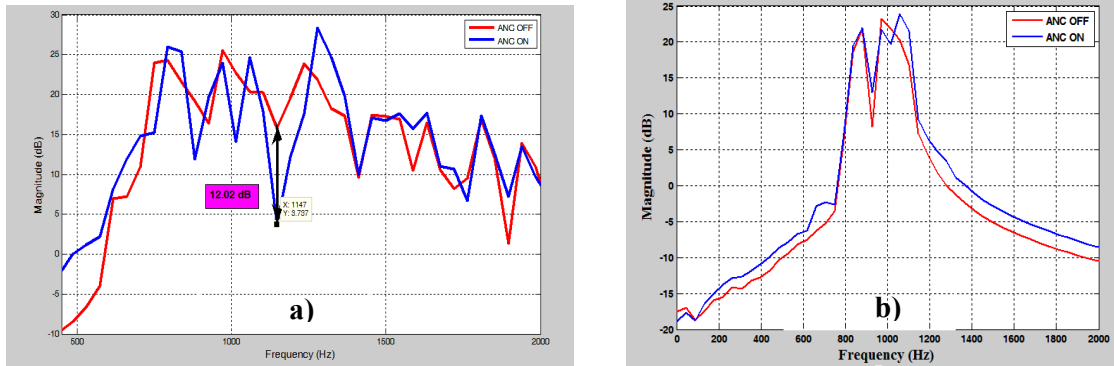


Figure 12. The system performance for band-width a) 500 to 2000 Hz b) 600 to 800 Hz.

On the other hand, as measured data shows 500 to 2000 Hz (Fig. 12(a)) contains the powerful frequencies. Table. 2 shows the attenuation magnitude in powerful frequencies. It is stated that the noise attenuation up to 12 dB was achieved.

Table 2. The system performance in noise attenuation for some frequencies.

Frequency (Hz)	749.7	882	1014	1147
Attenuation (dB)	8.7	7.3	8.5	12.01

5. Conclusion

In this paper, acoustical data were taken at IRIB data center to determine the noise characteristics and these were also used to find the powerful frequencies to regard as working frequency. The results showed that 500 to 2000 Hz band-width had significant SPL. These data were used in computational modelling of active noise control as well. The simulation results of 5×4×1 ANC structure based on FxLMS algorithm by using the measured data indicated that ANC was effective to attenuate the noise up to 12 dB.

REFERENCES

- Dunlap K, Rasmussen N. Choosing between Room, Row, and Rack-based Cooling for Data Centers. APC UK Co. (2014). [Online.]: <http://www.ithound.com/abstract/choosing-row-rack-cooling-centers-19884>
- Sommerfeldt, S. et-al, Feasibility Report, Brigham Young University, Acoustical Analysis of Active Control in the Server Room of a C7 Data Centers Colocation Facility, (2010).
- Sen, M.Kuo and Dennis, R. Morgan, *Active Noise Control Systems, Algorithms and DSP Implementations*, John Wiley & Sons, (1996).
- Sen, M. Kuo and Dennis, R. Morgan, Active Noise Control: A Tutorial Review, *Proceeding Of the IEEE*, June, (1999).
- ThomaKletschkowski, *Adaptive Feed-Forward control of low frequency interior Noise*, Springer, (2012).
- [Online.]: http://www.bksv.com/doc/prodcat/2260_Investigatior.pdf
- [Online.]: <http://recordinghacks.com/microphones/AKG-Acoustics/D-880>
- [Online.]: http://www.jr.com/neumann/pe/NM1_U87AI/
- [Online.]: http://www.maudio.com/images/global/manuals/051130_ProjMix_UG_EN01.pdf
- [Online.]: http://www.bruel.ru/UserFiles/File/4295_4296.pdf
- [Online.]: http://www.floralimited.com/images/PDF/Vostro_1320_1520_1720_Brochure.pdf
- Ljung,L. *System Identification Theory for User*, Practice Hall, (1997).
- The mathwork Inc., (2009).
- Welch, P.D, The Use of Fast Fourier Transform for Estimation of Power Spectra: A Method Based on Time Averaging Over Short, Modified Periodograms, *IEEE Trans. Audio Electroacoustics*, **15**(2), 70-73, (1967).